



1971

Calculation of levels of relative contribution of the carbon-dioxide channel radiance from TIROS VII in the case of a large-scale stratospheric warming in January 1964.

Giaque, Larry Lee.



Calhoun is a project of the Dudley Knox Library at NPS, furthering the precepts and goals of open government and government transparency. All information contained herein has been approved for release by the NPS Public Affairs Officer.

**Dudley Knox Library / Naval Postgraduate School
411 Dyer Road / 1 University Circle
Monterey, California USA 93943**

CALCULATION OF LEVELS OF
RELATIVE CONTRIBUTION OF THE
CARBON-DIOXIDE CHANNEL RADIANCE
FROM TIROS VII IN THE CASE OF A
LARGE SCALE STRATOSPHERIC
WARMING IN JANUARY 1964

LARRY LEE GIAUQUE

LIBRARY
NAVAL POSTGRADUATE SCHOOL
MONTEREY, CALIF. 93940

United States Naval Postgraduate School



LIBRARY
NAVAL POSTGRADUATE SCHOOL
MONTEREY, CALIF. 93940

THE SIS

CALCULATION OF LEVELS OF RELATIVE CONTRIBUTION
OF THE CARBON-DIOXIDE CHANNEL RADIANCE FROM
TIROS VII IN THE CASE OF A LARGE-SCALE
STRATOSPHERIC WARMING IN JANUARY 1964

by

Larry Lee Giauque

Thesis Advisor:

F. L. Martin

September 1971

Approved for public release; distribution unlimited.

LIBRARY
NAVAL POSTGRADUATE SCHOOL
MONTEREY, CALIF.. 93940

Calculation of Levels of Relative Contribution of the
Carbon-dioxide Channel Radiance from TIROS VII in the Case of
a Large-scale Stratospheric Warming in January 1964

by

Larry Lee Giaque
Lieutenant Commander, United States Navy
B.A., University of Colorado, 1961

Submitted in partial fulfillment of the
requirements for the degree of

MASTER OF SCIENCE IN METEOROLOGY

from the

NAVAL POSTGRADUATE SCHOOL
September 1971

ABSTRACT

A case study of a winter stratospheric warming in the western hemisphere in January 1964 between 60° and 40° north latitudes was conducted. Utilizing TIROS VII radiance data and analyzed height fields, a stepwise regression equation was determined to specify lower stratospheric layer temperatures. These temperatures were used with standard atmospheric temperatures to construct a sounding for use in a radiance computer program. Finally, this computed radiance was compared to regression values to determine if prediction and study of stratospheric warmings are valid and useful.

TABLE OF CONTENTS

I.	INTRODUCTION	9
II.	DATA PROCESSING	12
III.	STATISTICAL PROCEDURES AND INTERPRETATIONS	14
	A. DEFINITION OF DATA SETS	14
	B. TEST OF AN INDEPENDENT DATA SAMPLE	16
	C. STATISTICAL INFERENCES OF THE TEST	18
	D. CONSTRUCTION OF WARM AND COLD MODEL STRATOSPHERES	21
IV.	A NUMERICAL RADIATIVE COMPUTATION	26
V.	CONCLUSIONS	37
	APPENDIX - Computer Program	38
	LIST OF REFERENCES	59
	INITIAL DISTRIBUTION LIST	60
	FORM DD 1473	61

LIST OF TABLES

I.	Substratifications of sample data	14
II.	Stepwise order of entry of variables in the regression equation 4, including F_k upon-entry at step k , the test statistic <u>Critical</u> F_k^c , and multiple correlation co- efficient R_k at each step	16
III.	Comparison of explained variance between the dependent sample and independent sample	17
IV.	Means and standard deviations of $15\text{-}\mu$ temperatures and predictor thicknesses for samples $S_W(15)$ and $S_K(15)$	20
V.	Layer mean statistics for the warm and cold cases $S_W(15)$ and $S_K(15)$	21
VI.	Comparison of 10 mb temperatures of the warm and cold models to those of the standard atmosphere	22
VII.	Comparison of $15\text{-}\mu$ temperature computed from the sample mean and the model atmosphere radiance calculations	30

LIST OF FIGURES

1.	Warm and cold model atmospheres	23
2.	Proposed model warm atmospheric sounding	28
3.	Proposed model cold atmospheric sounding	29
4.	Carbon-dioxide channel radiance contributions for equal increments of $\ln p$ (warm model atmosphere)	32
5.	Carbon-dioxide channel radiance contributions for equal increments of $\ln p$ (cold model atmosphere)	33
6.	Warm case equal area weighting curve corresponding to Figure 4	34
7.	Cold case equal area weighting curve corresponding to Figure 5	35

TABLE OF SYMBOLS AND ABBREVIATIONS

A_i	Regression coefficients
$B(\lambda, T)$	Planck intensity function at wave length λ and temperature T
CO_2	Carbon dioxide
C	Degrees Celsius
F_k	F-ratio upon entry at step k
g	Acceleration of gravity
GMT	Greenwich Mean Time
I_λ	Outgoing monochromatic radiance
K	Degrees Kelvin
km	Kilometer
m	Meter
mb	Millibars
N	Detected radiance
p	Atmospheric pressure
q	Specific constituent mixing ratio
R	Multiple regression coefficient
R_d	Dry air gas constant
$S_W(10)$	Warm hemisphere sample of 10 January 1964
$S_K(10)$	Cold hemisphere sample of 10 January 1964
$S_W(15)$	Warm hemisphere sample of 15 January 1964
$S_K(15)$	Cold hemisphere sample of 15 January 1964
T	Temperature
X_i	Regression predictors
Y	Regression predictand

\hat{Y}	Regression predictand test values
ψ	Weighting function as a function of $\ln p$
h	Height above mean sea level
$\tau(h)$	Transmittance of the atmosphere to the outgoing $15\text{-}\mu$ band of CO_2 , between the levels $Z = h$ and $Z = \infty$
ϕ_λ	Filter function centered at wavelength λ , spanning the increment $\Delta\lambda$
λ	Wavelength
μ	Microns, identical to 10^{-4} cms
ΔZ	Thickness of atmospheric layer
$1-\alpha$	The significance of the predictor added expressed as a probability

ACKNOWLEDGEMENTS

The author wishes to express his appreciation to his advisor, Professor F. L. Martin, for his suggestions, advice, guidance and support in this research.

Appreciation is also expressed to the W. R. Church Computer Facility of the Naval Postgraduate School.

I. INTRODUCTION

The launch of the TIROS VII meteorological satellite on 19 June 1963 led to the remote sensing of stratospheric temperatures on a quasi-global scale. The orbits of TIROS VII were almost circular and had an average height of 635 km. The plane of the satellite orbit was inclined to the equatorial plane at an angle 58° , which resulted in scan-coverage between 60° north and 60° south latitudes. TIROS VII was equipped with a five-channel scanning radiometer, one of which measured the filtered thermal radiation of CO_2 in the half-power wavelength range 14.8 to 15.5μ [Staff members, 1964]. The CO_2 in the stratosphere should emit at the same temperature as the air (of which it is a part), thus the observed intensities can be interpreted in terms of a weighted-mean, equivalent black-body temperature in the stratosphere. Radiation transfer theory leads to the radiance from the 15- μ band [Warnecke, 1967] as

$$N_{15} = \int_{\lambda_1}^{\lambda_2} \int_{p=1000}^{p=0.1} \Phi(\lambda) \frac{\partial \tau(\lambda, \ln p)}{\partial (\ln p)} B(\lambda, T(\ln p)) d(\ln p) d\lambda \quad (1)$$

In (1), the 15- μ band is assumed opaque to the surface radiation. If the weighting function $\psi(\ln p)$ is defined as

$$\psi(\ln p) = \int_{\lambda_1}^{\lambda_2} \Phi(\lambda) B(\lambda, T(\ln p)) \frac{\partial \tau(\lambda, \ln p)}{\partial (\ln p)} d\lambda \quad (2)$$

the integral (1) reduces to

$$N_{15} = \int_{p=0.1}^{p=1000} [\psi (\ln p)] d (\ln p) \quad (3)$$

Thus the contribution of each layer to the radiance, N , sensed by the radiometer can be determined as a function of pressure. Radiative transfer theory applied to model atmospheres by Nordberg et al. [1965] indicates that maximum radiation, $\psi (\ln p)$, in the 15- μ range is emitted by the low stratosphere. The maximum weighting contribution at small nadir angles originates at about 25 km but the 15- μ temperature corresponds to different heights from time to time because the temperature structure in the stratosphere changes with time [Belmont et al., 1968]. Radiance should also then be statistically related to the mean temperature or thickness between various pressure levels in the stratosphere. The latter conjecture was the originating hypothesis of this investigation.

Several studies have appeared in the literature which strongly support a relationship with 15- μ temperatures at pressure levels in the stratosphere. Belmont et al. [1968], Nordberg et al. [1965], Warnecke [1967] and Teweles [1966] indicated that 15- μ temperatures depict some of the large scale horizontal wave activity in the thermal fields of the lower stratosphere. In addition, Kennedy [1966], has compiled an atlas of ten-day mean isotherm charts recorded by the 15- μ channel of TIROS VII for the period June 1963 through July 1964. These charts were presented by Kennedy as indicative of the spatial temperature distribution of the lower stratosphere during the total period of analysis of TIROS VII. Between 60° north and 60° south

latitudes these charts depict, for example, the proper seasonal distribution of stratospheric isotherms at about 25 km.

Dense cloud bands will cause a decrease in the $15\text{-}\mu$ temperature and will raise the peak elevation of its radiance weighting function. Although data presented in the Kennedy Atlas were not corrected for cloud contamination, nevertheless, the reduction to ten-day mean $15\text{-}\mu$ temperatures was considered by Kennedy to have eliminated the cloud contamination effect. This atlas served as a source for grid point $15\text{-}\mu$ temperature data for the case studies investigated in this dissertation.

Since the $15\text{-}\mu$ temperatures are weighted over an indefinite thickness range in the stratosphere, Belmont et al. [1968] has raised the question, "which pressure level in the stratosphere does the $15\text{-}\mu$ temperature best represent?" Moreover, Shen et al. [1968] have shown the usefulness of $15\text{-}\mu$ temperature fields in detecting stratospheric warming events in the Southern Hemisphere polar winter. This paper seeks to relate statistically the various layer-contributions to the $15\text{-}\mu$ temperature in the case of a winter stratospheric warming in the polar latitudes of the Western Hemisphere. This case was centered time-wise on 15 January 1964.

II. DATA PROCESSING

The 15- μ temperatures were extracted from the Kennedy Atlas [1966] of stratospheric mean 15- μ isotherms, using charts 42 (10 January 1964) and 43 (15 January 1964). Grid points values for 60 $^{\circ}$, 50 $^{\circ}$, and 40 $^{\circ}$ north and every 5 $^{\circ}$ of longitude around the globe were carefully interpolated to the nearest whole degree Kelvin. These 216 grid points were further divided into two hemispheres: that between 70 $^{\circ}$ west and 110 $^{\circ}$ east longitude corresponding to the "cold" sample since it approximated the sector of the winter cold vortex. The "warm" hemisphere between 110 $^{\circ}$ east and 70 $^{\circ}$ west longitude (the "Western" Hemisphere) contained the warm stratospheric anticyclone. There were 108 grid points located in each sample.

Thickness values at each of the 216 grid points were noted and for both dates of interest were determined from the Northern Hemisphere analyses of 10, 30, 50, 100 and 300 mb contour charts. These charts were found in the January 1964 series of map analyses of the Institute of Meteorology and Geophysics of the Free University of Berlin [1964]. Contour values from each pressure level and at each grid point were differenced to determine four thicknesses in the stratosphere and upper troposphere:

10 - 30 mb thickness, denoted $X_1(i,j)$

30 - 50 mb thickness, denoted $X_2(i,j)$

50 - 100 mb thickness, denoted $X_3(i,j)$

100 - 300 mb thickness, denoted $X_4(i,j)$

Finally, the dependent variable is the 15- μ temperature and is denoted hereafter as $Y(i,j)$.

The statistical model is then to be expressed in the multiple-regression form

$$Y = A_0 + A_1X_1 + A_2X_2 + A_3X_3 + A_4X_4 \quad (4)$$

where the coefficients A_0 , A_1 , A_2 , A_3 and A_4 are to be determined by the least squares techniques. All of the variables for input into equation (4) were encoded onto punched cards in a format consistent with the requirements of the stepwise regression program, BMD02R [Dixon, 1966]. This program is available in the Library of the W. R. Church Computer Center of the Naval Postgraduate School.

III. STATISTICAL PROCEDURES AND INTERPRETATIONS

A. DEFINITION OF DATA SETS

As noted previously, it was necessary to stratify the data for the two map-times into cold and warm stratospheric "hemispheres". According to the stratospheric contour and temperature analyses of the Free University of Berlin, the warming anticyclone had reached its peak intensity in the Western Hemisphere on 15 January 1964, with a well-defined cold hemisphere adjacent. The stratospheric warming was still in a developing stage on 10 January 1964. This led to the four sub-stratifications of sample data, which for simplicity will be denoted in Table I.

TABLE I

Substratifications of Sample Data

Date	Warm	Cold
10 January	$S_W(10)$	$S_K(10)$
15 January	$S_W(15)$	$S_K(15)$

Actually the last two, $S_W(15)$ and $S_K(15)$ were used to generate the multiple regression equations of type applicable to the warm and cold hemispheres, respectively. These equations were then to be tested for diagnostic significance by applying them to the independent samples $S_W(10)$ and $S_K(10)$. Each of the four stratifications had 108 data sample sets.

The BMD02R regression analysis not only generates a multiple regression equation similar to (4) but also performs a step-wise

screening in the process: it first determines that independent variable X_i which explains the highest percentage variance of Y . Then at step two, it determines the X_j in the remaining predictor set that explains the largest percentage of the residual variance unexplained by the first variable, and so forth, for steps three and four.

The BMD02R program also computes for each step the F-statistic upon-entry of the k th variable selected, where F_k is expressible at step k as [Dixon, 1966]

$$F_k(1, n-k-1) = \left[\frac{(\% \text{ cum. expl. var., step } k) - (\% \text{ cum. expl. var., step } k-1)}{(\% \text{ unexplained variance at step } k)} \right]$$

In the present problem, two tests were to be made using X_1 , X_2 , X_3 and X_4 with a total sample size of $n=108$ in the warm and cold cases $S_W(15)$ and $S_K(15)$, respectively. Based upon the magnitude of F_k of (5), Table II indicates the order of entry of the predictors selected and the corresponding F_k -statistic with which they entered.

For each predictor tested, its significance at step k may be assessed by comparison of its F_k value with a Critical F_k^C defined after Miller [1962] as

$$F_k^C = F_{\alpha/p-k+1}(1, n-k-1), \alpha = 0.05 \quad (6)$$

in order that the over all regression be assured of significance at the $1-\alpha$ confidence level. The set of Critical F_k^C values to be used for comparison are adjoined to Table II.

The four-predictor regression equations having the form of (4) are as follows:

$$S_W(15), Y = 112.213 - .04842X_1 + .03686X_2 + .18648X_3 + .07498X_4 \quad (7)$$

TABLE II

Stepwise order of entry of variables in the regression equation (4), including F_k upon-entry at step k, the test statistic $\text{Critical } F_k^c$, and multiple correlation coefficient R_k at each step

Sample-Warm, $S_W(15)$, $n=108$				Sample-Cold, $S_K(15)$, $n=108$			Critical Values F_k^c
Step No.	Variable entering	F_k	Mult. Corr. Coeff.	Variable entering	F_k	Mult. Corr. Coeff.	
k=1	X_3	179.13	.7926	X_3	14.81	.4252	6.51
2	X_1	54.20	.8688	X_1	8.42	.4905	6.00
3	X_4	39.20	.9066	X_4	4.21	.5083	5.19
4	X_2	4.36	.9106	X_2	1.72	.5201	3.96

$$S_K(15), Y=171.927 + .04872X_1 + .06728X_2 + .10750X_3 - .07642X_4 \quad (8)$$

Table II shows that all thickness predictors entered at a confidence level of 95 percent for each entry in equation (7). On the other hand, for the cold case, the order of entry was identical to that of $S_W(15)$ but the levels of significance for X_4 and X_2 were subcritical. However, in the cold case, the standard error of estimate continued to decrease from step three to step four, so the full four predictor equation (8) was retained for testing against the independent sample $S_K(10)$. A more complete justification for retaining the full set of predictors can be found at the end of III-C.

B. TEST ON AN INDEPENDENT DATA SAMPLE

In order to test the validity of equations (7) and (8) developed from $S_W(15)$ and $S_K(15)$, the coefficients from these samples were

combined through the matrix multiplication (9) to form the estimator-predictand of the independent data

$$\hat{Y} = (A_0, A_1, A_2, A_3, A_4) \begin{pmatrix} 1 \\ X_1 \\ X_2 \\ X_3 \\ X_4 \end{pmatrix} \quad (9)$$

using the sets $S_W(10)$ and $S_K(10)$. The regression between (Y,Y) for the independent sample gave the results listed in Table III as compared to the dependent case.

TABLE III

Comparison of explained variance between
the dependent sample and independent sample

Dependent Sample		Independent Sample		
	% Expl. Variance	% Expl. Variance	R(Y,Y)	$F_1(1,106)$
S_W	82.92	47.11	.6864	94.426
S_K	27.05	76.61	.8753	347.266

There was a sizeable shrinkage in explained variance in the warm case when applying the regression from the $S_W(15)$ case to the independent data set. However, in this case the F-test still indicated confidence well over the 95 percent level of belief in spite of the shrinkage. The result of the regression for the cold case showed a significant improvement in the explained variance of T_{15} in the independent sample, an unexpected result which will be discussed below.

C. STATISTICAL INFERENCES OF THE TEST

The stratospheric warming which seemed to reach its maximum magnitude over the entire "warm" hemisphere on 15 January, had also spread to some extent into the "cold" hemisphere. The fact that the warming process had encompassed the entire warm sector and a part of the cold sector may explain the wide range of explained variance between the two sectors on 15 January including the rather low explained variance in $S_K(15)$.

A statistical reason for the observed shrinkage in explained variance in passing from the dependent equation (7) to the independent sample of 10 January may be ascribed to the incomplete development of the full warm hemisphere as of this date, so that the sample of 10 January actually consisted of a mixture of warm and cold data points. In other words, the warm hemisphere of 10 January seems not to have been as clearly stratified as a warm hemisphere as that of 15 January.

The phenomenon of an increased percentage explained variance in passing from equation (8) to the independent cold sample of 10 January was subject to a similar conjecture. The relatively small multiple regression coefficient resulting from $S_K(15)$ seemed to indicate that a stratospheric warming effect had also begun to spread into the "cold" hemisphere, and in consequence only 27.05 percent of the variance of Y was explained by the specification equation (8). On the other hand, the much larger percentage of the variance explained by (8) applied to $S_K(10)$ seems to indicate that the cold stratification for the 10 January case was more uniform than the dependent case chosen for 15 January.

In retrospect, a more flexible sampling procedure which might have improved the results should have involved more care in delineating the stratifications of the areas of warm and cold stratospheres, respectively. For example, it now seems reasonable to limit the warm area sample to those stratospheric grid points having anti-cyclonic contour curvature and not necessarily assigning an entire hemisphere to the sample. Similar considerations, with regard to cyclonic curvature might well have afforded a better criterion for the cold stratification in both the dependent and independent cases.

It was now possible to offer a more complete statistical reason for retaining all four predictors in the right side of equation (8). Even though the dependent cold sample from which equation (8) was derived seems to have been not uniformly stratified, the use of the resulting predictand was well verified ($R(Y, \hat{Y}) = .8753$) on the more stable stratified cold hemisphere of 10 January.

It was also noteworthy that a choice of $S_K(10)$ as the dependent cold sample gave the same order of entry for variables as indicated in Table II, with all individual predictors significant at well above the 95 percent confidence limit.

With \hat{Y} based upon equation (8), the ensuing regression between \hat{Y} and Y for 10 January was

$$\hat{Y} = -95.3142 + 1.4298\hat{Y}, R(Y, \hat{Y}) = .8753 \quad (10)$$

so that by equation (10) all predictors would have had the same coefficient matrix apart from the constant multiplier, 1.4298.

Thus equations (7) and (8) are adopted as the representative regression equations for the warm and cold stratospheric samples, respectively.

Since the regression equations just listed must be satisfied by the sample means, it is useful to list the mean properties of these two atmospheric samples $S_W(15)$ and $S_K(15)$. Table IV is a compilation of the means and standard deviations of all variables which appear in equations (7) and (8) for 15 January 1964.

TABLE IV

Means and standard deviations of 15- μ temperatures and predictor thicknesses for samples $S_W(15)$ and $S_K(15)$

Vrbl.	$S_W(15)$		$S_K(15)$	
	Mean	Std. Dev.	Mean	Std. Dev.
T_{15}	226.16K	3.68923	217.96K	4.79275
X_1	7298.1 gpm	327.7286	6796.5 gpm	268.4886
X_2	3356.1	126.8544	3149.4	100.4864
X_3	4520.6	165.8544	4221.9	162.5060
X_4	7017.0	125.0733	6998.1	138.5645
Y	226.16K		217.96K	

The standard deviation of X_1 (the 10 to 30 mb thickness) was considerably larger than the other levels; however, it is a layer subject to more radiosonde error than those below it. Also interpolation of contour height to grid points was more subjective at 10 mb due to stronger gradients than existed at lower levels in the stratosphere.

Because of the equivalence of thickness to mean temperature of an isobaric layer through the integrated form of the hydrostatic equation

$$\Delta Z = \frac{R_d}{g} \ln \frac{p_1}{p_2} \bar{T} \quad (11)$$

it is possible to ascribe a mean temperature to each of the four isobaric layers of thicknesses hitherto denoted X_1 , X_2 , X_3 and X_4 . These mean temperatures corresponding to the mean thicknesses already listed in Table IV are given in Table V for the warm and cold stratospheres respectively, along with other relevant statistics used in the specification of the 15- μ temperature. The statistic $R(Y, X_i)$ is the simple correlation between T_{15} and the i th layer-thickness.

TABLE V

Layer mean statistics for the warm and cold cases $S_W(15)$ and $S_K(15)$

			Warm Case		Cold Case	
	Layer (mb)	Mid- point press.	$R(Y, X_i)$	Layer mean temp.	$R(Y, X_i)$	Layer mean temp.
X_1 :	10 - 30	17.32 mb	.195	226.96K	.750	211.36K
X_2 :	30 - 50	38.73	.663	224.40	.281	210.56
X_3 :	50 - 100	70.71	.793	222.82	.161	208.09
X_4 :	100 - 300	173.20	.656	218.22	-.340	217.63

D. CONSTRUCTION OF WARM AND COLD MODEL STRATOSPHERES

From the mean temperatures listed in Table V, stratospheric model temperature-pressure distributions were constructed for the warm and cold cases in Figure 1: A-B-C-D showing the lower stratosphere temperatures in the warm case and A'-B'-C'-D' showing the lower stratosphere temperatures in the cold case at 17.3, 38.7, 70.7 and 173.2 mb

respectively. The lowest points D and D' lie within a half degree Celsius of one another, at the 173.2 mb level.

Since no mean temperatures were available from this study below 173.2 mb, the cold and warm cases were adjoined to the Cold and Warm Supplemental Standard Atmospheres [Dubin et al., 1966] at latitude 60° north in January. The cold and warm January standard profiles below 300 mb were virtually identical and for the purpose of the modeling done here were taken as the unique curve E-F-G in Figure 1. This led to a minor inconsistency in the mean temperatures to be expected in the layer 100-300 mb in the cold and warm cases, respectively.

The expected temperature at 10 mb for the warm and cold models were obtained by extrapolating the lines B - A and B' - A' in Figure 1 to the 10 mb level. This technique led to the results listed in Table VI:

TABLE VI

Comparison of 10 mb temperatures of the warm and cold models to those of the January Supplemental Standard Atmosphere (60° north)

	Warm	Cold
10 mb, model	-43.65C	-61.15C
Jan. 60N Supp.	-43.75C	-73.50C

It is clear that the lower stratospheric temperatures from the warm sample are in good agreement with the January warm standard, while the cold sample was not as clearly definitive of the cold standard for the reasons already cited in III-C.

The remainder of the model above the 10 mb level was fitted in both models by extending linearly the T-ln p profile from 10 mb upward to

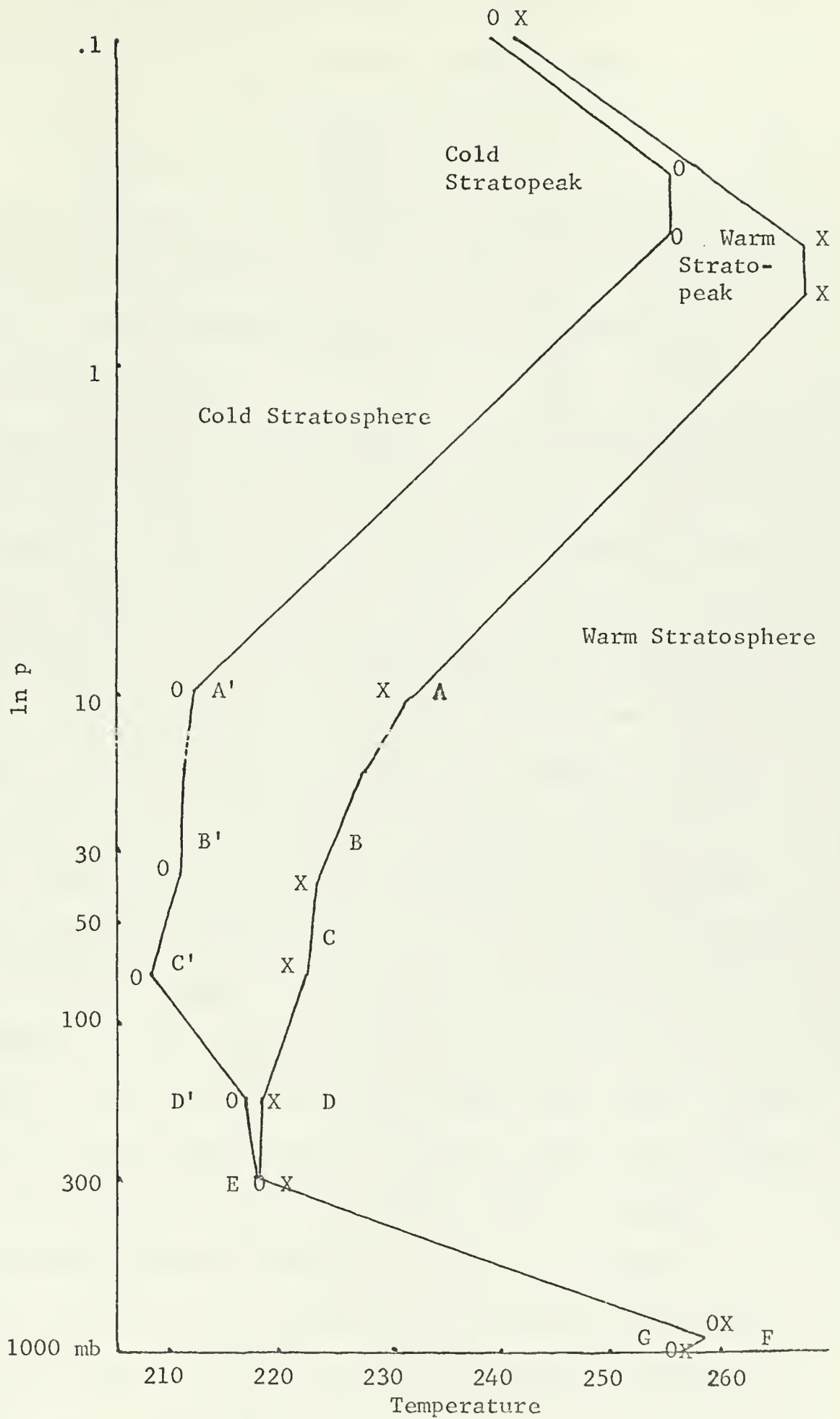


Fig. 1. Warm and cold model atmospheres

the listed stratopeaks of the Warm and Cold Supplemental Standards [Dubin et al., 1966]. These peaks occur over the range:

$$p = 0.7 \text{ to } 0.423 \text{ mb where } T = -5\text{C}$$

$$p = 0.44 \text{ to } 0.26 \text{ mb where } T = -17\text{C}$$

Above the top of these levels, the listed lapse rate above the stratopeak was used to extend the $T-\ln p$ models to the level $p=0.1$ mb, which is commonly taken as the top of the atmosphere in radiative-transfer theory.

The simple correlation coefficients listed in Table V give some indication of the layers contributing most heavily to the specification of T_{15} . The results in the warm case (Table V) indicate a maximum influence or weight from the layer 50-100 mb centered at 18.1 km (70 mb). However, there is considerable additional influence from the 30-50 mb and 100-300 mb layers (at 26.4 and 12.2 km, respectively). Note that the influence from the layers X_2 , X_3 and X_4 as indicated by $R(Y, X_i)$ seem significant. This will be discussed further in IV.

On the other hand, the cold model atmosphere has the maximum influence detectable from this study in view of the high correlation coefficient $R(Y, X_1)$, (Table V), attributable to the layer 10-30 mb and this influence decreases systematically below this level. The significant negative correlation in the lowest level (100-300 mb) is apparently due to the low warm tropopause which is synoptically expected with a cold stratospheric vortex situation. The overlying deep cold layer (100-10 mb) apparently acts as an effective absorber, and relatively low-emittance re-radiator of the CO_2 radiation started in the high troposphere. In other words, this negative correlation in the lowest layer is apparently related to the relatively steep lapse

rate between the lowest part of the stratosphere and the warm tropospheric layer immediately below.

IV. A NUMERICAL RADIATIVE COMPUTATION

A brief discussion of the upwelling radiance from an arbitrary planetary atmosphere having a temperature distribution $T = T(p)$ and constituent distributions $q_i = q_i(p)$, $i=1, \dots, 3$, is given. V. Kunde [1967] prepared a detailed theoretical study of a number of planetary atmospheres detailing the necessary theoretical computations for the upwelling radiances sensed by various medium resolution infrared radiometers. Kunde's theory [Kunde, 1967] made use of spherically horizontal symmetry of all sounding properties in the atmosphere, and computed the transmitted radiative contributions from each level p to $p+dp$. Thus he made use of the generalized formula for outgoing radiance

$$dI_\lambda = B_\lambda [\lambda, T(\ln p)] \frac{d\tau}{d(\ln p)} d(\ln p) \quad (12)$$

in the case of a satellite sensor having optical filter response $\Phi_\lambda = 1.0$. In equation (12), the transmittance τ is the constituent product-transmissivity at pressure p , and τ must be a decreasing function of pressure. The Curtis-Godson approximation is used for correcting the vertical absorber mass distribution, and for deducing the resultant pressure-effect upon line broadening.

When CO_2 is the main emitter and the earth's 15- μ band the main source of outgoing radiation, the surface may be considered black in the terrestrial spectrum (reflectivity zero). The problem was further simplified by assumed constancy of the mixing ratio of CO_2 at $q = 0.477$ gm/kg. The details of the vertical variation of water vapor and ozone mixing ratios, which are highly variable for each gas, were supplied in the form of a sounding distribution of each. These

gases are distributed relative to height or, equivalently to the pressure $p = p(h, T)$.

Based on the results of III-D, two model vertical profiles $T(p)$ were determined from Figure 1 with sufficient vertical resolution (about thirty significant levels) to cover the entire range of pressure from $p = 1013.5$ mb to $p = 0.1$ mb, for both the warm and cold cases in Figures 2 and 3.

The vertical distributions of water vapor and ozone enter the computation of N_{15} only in a very secondary manner since there is only slight overlap between the water vapor rotational band wings and the $14.0\text{--}16.3\mu$ response function placed upon the sensors of the $15\text{-}\mu$ channel of TIROS VII. The sensor response function $\Phi(\lambda_j)$ associated with the j th subinterval, $\Delta\lambda_j$, of the $15\text{-}\mu$ channel are listed in the TIROS VII Radiation Data Catalog and Users' Manual [Staff, 1965].

The water vapor and ozone mixing ratio distributions with height actually used were listed for Maniwaki, Quebec (46N, 76W) based upon the real time radiosonde observations taken on 29 September 1958 at 1200 GMT. The Maniwaki surface values (at 996.0 mb) of mixing ratio were considered identical to those at 1013.5 mb of the present models atmospheric base level.

The integral $\psi(\ln p)$ of equation (2) represents the contribution to the total filtered radiance at a point in space in $\text{watts/m}^2/\text{ster}$ of depth and includes the Planck-Kirchhoff transmittance attributed to a small pressure increment dp , as essentially specified by the radiosonde (including the constituent mixing ratios).

The Kunde radiative transfer theory [Kunde, 1967] was applied to both of the model atmospheres as input, and with the model-invariant



Fig. 2. Proposed model warm atmospheric sounding

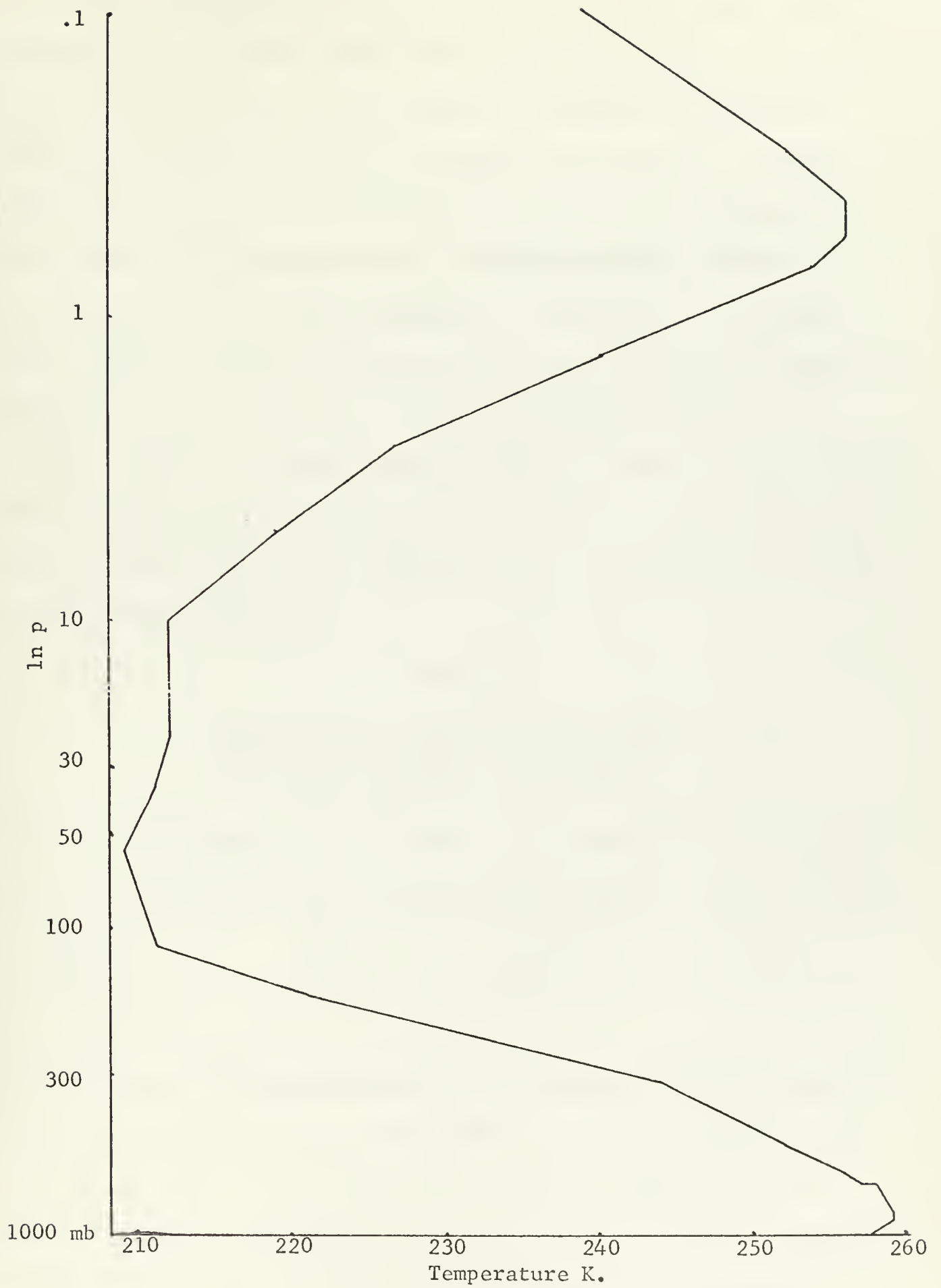


Fig. 3. Proposed model cold atmospheric sounding

mixing ratio distributions of $q_{H_2O}(p)$ and $q_{O_3}(p)$. The Kunde computer program is listed in the Appendix. The program was designed to give the total filtered N and the corresponding T_{15} computed by five-point interpolation from the laboratory calibration of N vs T_{15} . In this theoretical program no instrument degradation need be considered. Finally the first important output of the program gives N and the effective T_{15} for the model atmospheres. It also gives a pressure-height weighting function essentially equivalent to $\psi(\ln p) = dN/d(\ln p)$ appropriate to the contribution to N for equal increments of $\ln p$.

The results of the model-atmosphere radiance computation after Kunde [1967] applied to the warm and cold models (and the implied soundings, Figures 2 and 3) led to the following results for calculated N and the resultant 15- μ temperatures.

TABLE VII
Comparison of 15- μ temperature computed from the sample-mean and the model atmosphere radiance calculations

	N(watts/m ² /ster)	T_{15} [Kunde]	$\bar{T}_{15} = Y$
$S_W(15)$	3.048	228.9K	226.2K
$S_K(15)$	2.460	218.1K	217.9K

In Table VII the corresponding values are in columns 3 and 4, whereas the contrast between the model atmospheres is to be seen by comparing row 2 against row 3. It is to be noted that the warm case emits a greater N than the cold sample, and that the model atmospheres adopted reproduce the respective sample mean \bar{T}_{15} temperatures effectively.

Another important output of the Kunde program is the percentage of total N associated with increments of $\ln p$ between $p = 0.1$ and $p = 1013.5$ mb. This output was listed in the Kunde program by kilometer intervals and at equivalent pressure levels for the warm and cold model atmospheres and the results summed to give the weight functions $\psi(\ln p)$ in the form of block-diagrams on a $\ln p$ scale (Figures 4 and 5). These block diagrams were subsequently smoothed preserving equal areas of $\psi(\ln p)$ from block-to-block and the results appear as Figures 6 and 7.

It is now useful to reconsider the simple correlation coefficients between T_{15} (and therefore N), and the layer thicknesses given in Table V. For the cold atmosphere, the negative correlation attributable to the layer 100-300 mb has been explained by the compensating cool shielding layer C'B' which occurs even when a temperature rise occurs at or near 300 mb. However, the correlation coefficient of 0.750 between the 10-30 mb thickness and the total radiance was due to sampling variations in temperature of B'A' about the mean profile $T(p)$ of Figure 1, with a warmer than average upper layer able to contribute more radiance to space than if the layer were sampled as relatively cold. This result verifies the positive correlation $R(T_{15}, X_1) = 0.750$ found for the cold case.

A similar argument was applied to the warm case where the lapse rate from the upper troposphere to the stratopause was continuously of an inversion nature. Any layer sampled in $S_W(15)$, if warmer than the mean, tends to have greater emittance to space, whereas it will have smaller emittance when cooler than normal accounting for the positive correlations in Table V. This effect is especially prominent near the level of

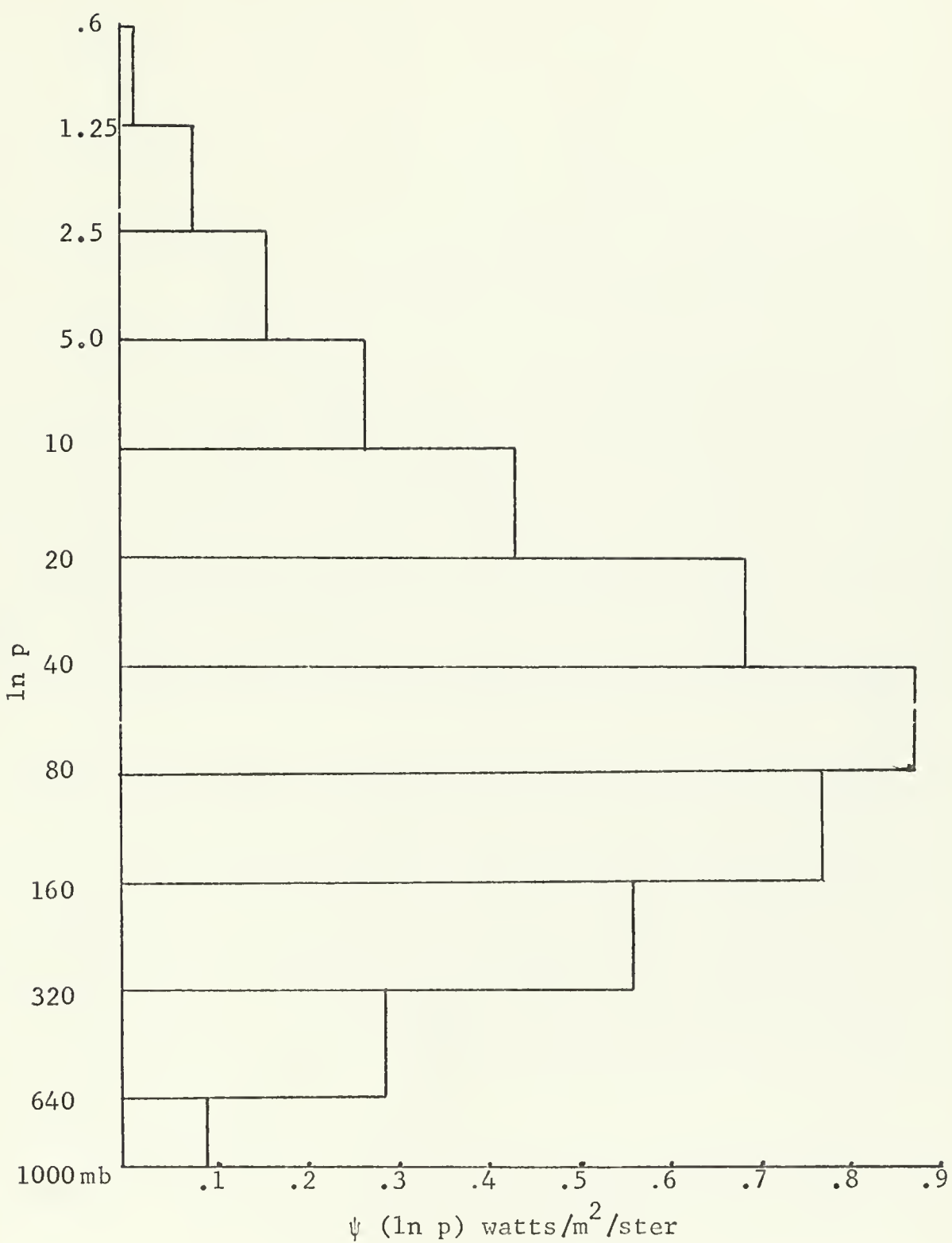


Fig. 4. Carbon-dioxide channel radiance contributions for equal increments of $\ln p$ (warm model atmosphere)

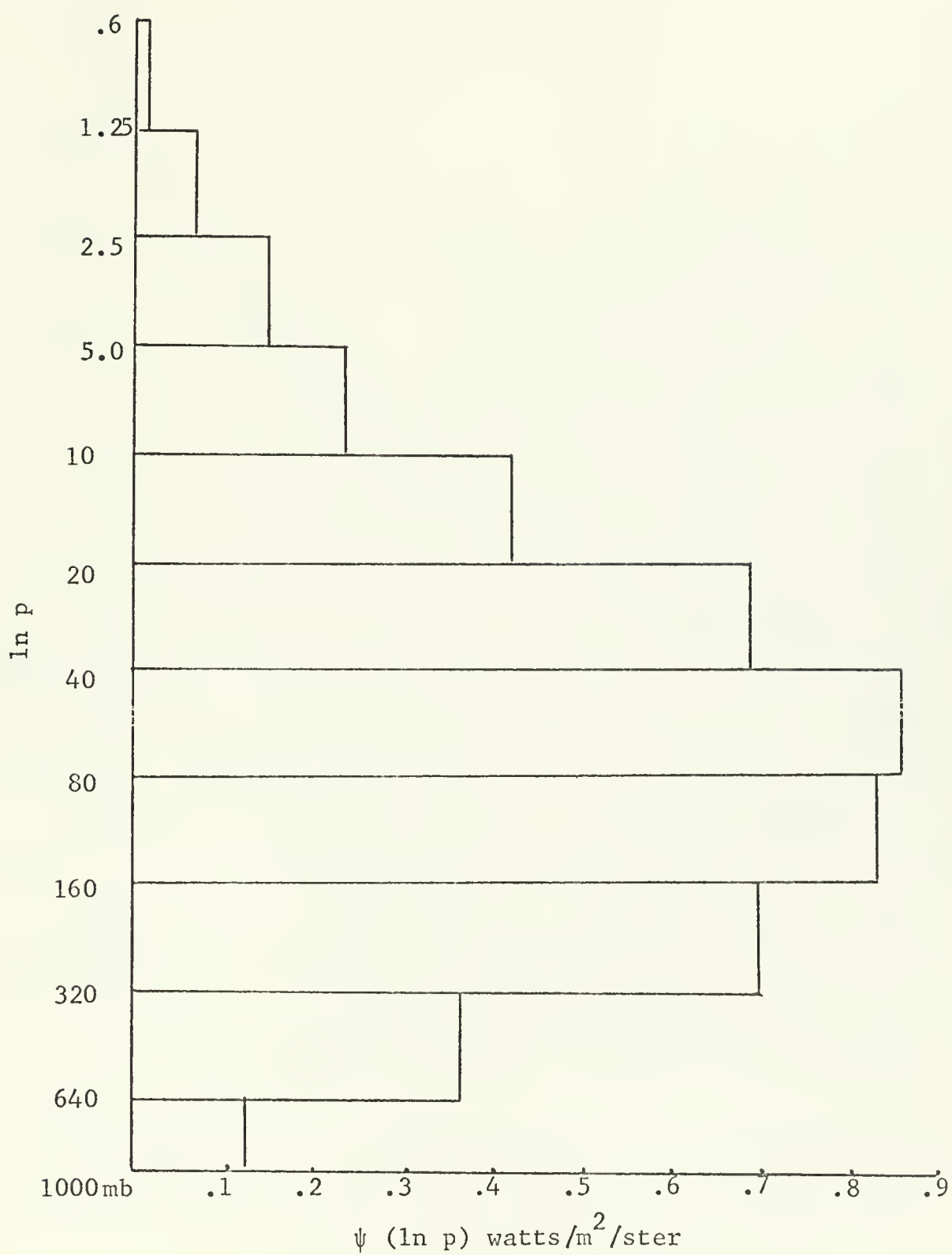


Fig. 5. Carbon-dioxide channel radiance contributions for equal increments of $\ln p$ (cold model atmosphere)

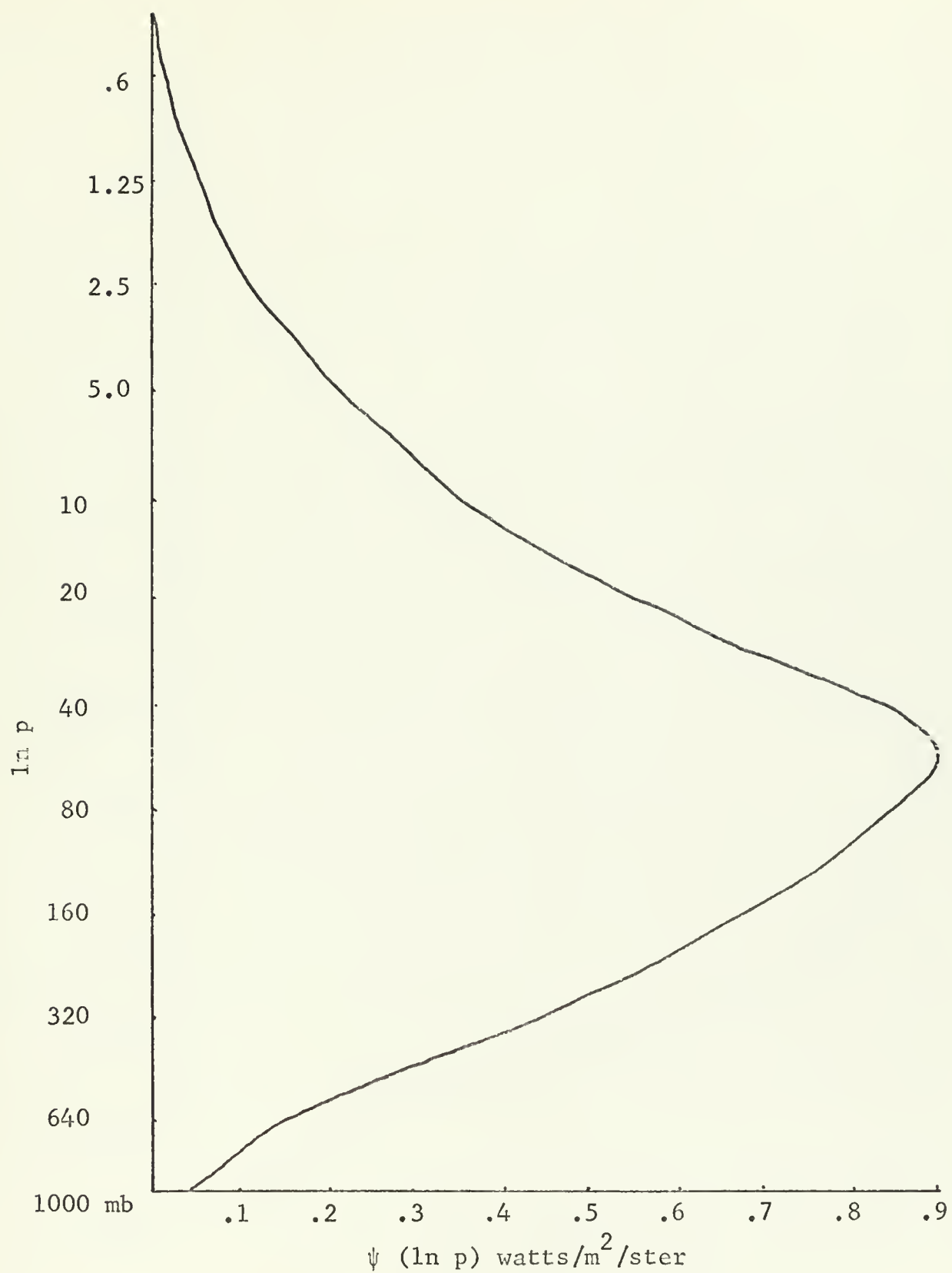


Fig. 6. Warm case equal area weighting curve corresponding to Fig. 4

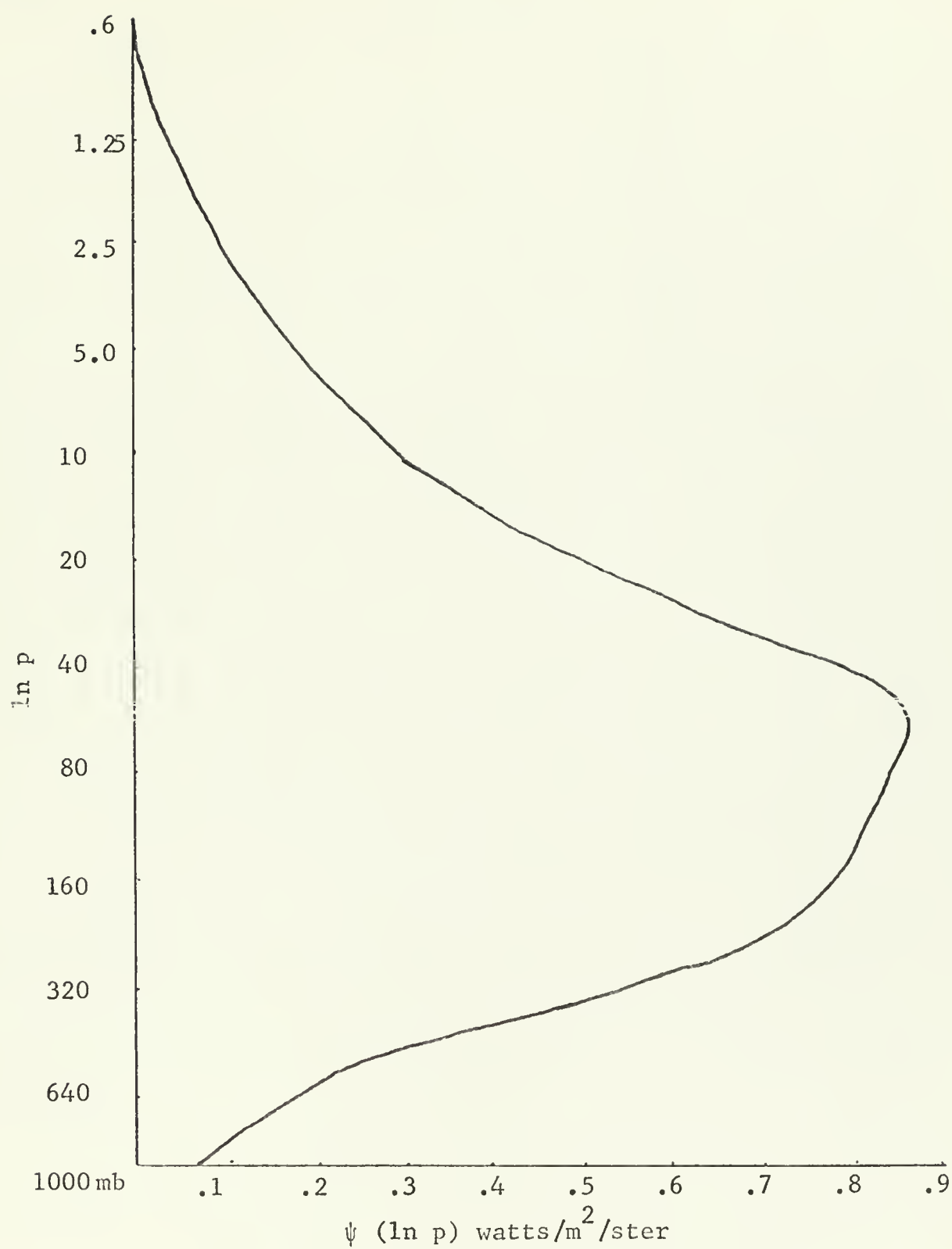


Fig. 7. Cold case equal area weighting curve corresponding to Fig. 5

maximum weighting function $\psi(\ln p)$, which occurs in the range 50-100 mb.

V. CONCLUSIONS

The results of this study of a northern hemisphere stratospheric warming indicate that a polar-orbiting satellite with a 15- μ sensor can be used as a tool to study stratospheric warming processes. The layers of the lower stratosphere which are initially affected can be identified by comparison of regression values to normal soundings for that of the anticyclonic area or the vortex area. Although this study was concerned only with one stratospheric warming, the correlation coefficients are large enough to seem significant. This was especially true in the $S_W(15)$ sample which was particularly well stratified with respect to the warming.

A daily synoptic analysis of the CO_2 channel radiance information from a polar-orbiting satellite should provide initial indications of when a stratospheric warming is beginning. The development of such a warming may easily be followed as it progresses around the globe. Future operational study in this area by use of smaller sectors, using successive-day swath continuity might allow enough data-definition to follow such a warming as it develops in the vertical and could become a tool for the study of stratospheric warmings.

APPENDIX

KUNDE RADIANCE PROGRAM FOR 15- μ BAND OF CO₂

```

COMMON/AA/WORDS(18), WAVEI,WAVEF,INTER,HT2,HT4,ANGLE,NUU,JTAN,LA
COMMON/TT/TRAN(500)
COMMON/GO,XMINH,PI,RAD,CAPK,C1,C2,DEL,DELHC,HT,XMAXH,HC,TO,IGAS,I
1  ATM/ZA/IXA,DATA(200)/ZB/IXB,DATB(100)/ZC/IXC,DATC(100)
COMMON/ZF/IXF,DATE(100)/ZF/IXF,DATE(100)/ZG/IXG,DATG(100)/ZH/IXH,
1  DATH(100)
COMMON/ZI/IXI,DATI(100)/ZJ/IXJ,DATJ(100)/ZK/IXK,DATK(100)/ZL/IXL,D
1  ATL(100)
COMMON/ZM/IXM,DATM(100)/ZN/IXN,DATN(200)
DIMENSION SUMHTU(1000),SUMHTL(1000),SUMLAY(1000)
DIMENSION PLKA(4),PLKB(4),PLKI(4),XTA(10,70,6)
DIMENSION XT2(1000),XPBOT(1000),UCQ2(1000),PCQ2(1000)
DIMENSION PRESS(100),TEMP(100),HH(100),HMIN(100),PRESH(100),PREHH(
1  100),XP(1000),XT1(1000),XDEL(1000),X(1000),XI(1000)
DIMENSION TRFM(500),TRH63(500),TRD96(500)
DIMENSION TROT(500),TPCON(500),TRCQ2(500)
DIMENSION WA(15),T1(75),T2(75),T3(75),T4(75),T5(75),T6(75),T7(75),
1  T8(75),T9(75),T10(75),T11(75),T12(75),T13(75),T14(75),T15(75)
DIMENSION CNHITEM(100),QH2Q(50),QH2Q2(50),HETH2Q(50),HETCQ2(50)
DIMENSION WAVEE(100),WAVEF(100),WAVEJ(100),WAVEK(100),
1  WAVEK(100),WAVEM(100),XLUVE(100),XLUH(100),XLUJ(100),XLUK(100)
DIMENSION TMIDIN(800),XINTIG(800),XLUU(100),XLUV(100),XLUW(100),
1  DIMENSION WAW(500),ANGLE(6)
DIMENSION HBOT(25),WAVSP(50),PHI(50),XNBAR(50),TEMPR8(50)
1  SPWCRP(18)
DIMENSION WAVEU(100),DATU(100),XLUU(100),DATUU(100),WAVEV(100),
1  DATV(100),XLUV(100),DATUV(100),TRH32(500),TRC43(500),TRCH33(500),
1  TRN2Q(300),UCH4(950),USCH4(950),UN2Q(950),USN2Q(950),WEE(100)
1  WAVEW(100)
FORMAT(13,13,13,(E13.7))
1  F12.4/27X,10X,F8.2,6X,F12.9,6X,F7.2,6X,F12.7,6X,F11.7,6X
1  F12.8X,F7.2,6X,1PE12.5,5X,1PE12.5,5X,OPF8.5,
2  6X,OPF12.4/27X,1PE13.6,5X,1PE13.6)
FORMAT(13)
FORMAT(10(5.2))
FORMAT(5(F3.1,F7.5))
FORMAT(1H,10X,3HH2C,4X,4HK = F11.7,3X,7H C1 = F4.2,3X,7H C2 = F
1  4.2)
FORMAT(13,13,13,(E13.7))
8  FORMAT(18A4)
FORMAT(1H,10X,8HANGLE = F6.2,3X,7HXMINH= F8.2,3X,26HLOWER INTEGRA
1  TION LIMIT = F7.2)
FORMAT(F5.2)
FORMAT(1H,4I5)
FORMAT(F6.2,13,(F10.6))
FORMAT(3F12.6,F6.2,F6.2,F6.2)
FORMAT(1H,10X,12HCASE NUMBER I3)

```



```

1 1ATH (LENGTH)
5620 1) FORMAT(1H ,5X,F7.3,3X,F7.2,3X,F8.4,3X,F9.4,5X,F8.4,4(1X,E10.4,1X)
5621 1) FORMAT(1H1,20X,49HALL QUANTITIES REFER TO BOTTOM OF LAYER CO2 GA
1S)
5622 1) FORMAT(1H ,20X,34HEXCEPT EFF PRESS AT LAYER MIDPOINT)
5624 1) FORMAT(1H0,26H15.0 MICRON CO2 GEN ABSORPT
5625 1) FORMAT(2F6.2)
5626 1) FORMAT(1H0,4,F10.2)
5627 1) FORMAT(1H ,5X,F10.2,3X,F12.6,3X,F10.4)
5628 1) FORMAT(1H ,3X,F10.2,4,3(2X,1PE10.4,1X),2PF10.4,F10.2,F8.2,2F10.4)
5629 1) FORMAT(1H1,20X,24HATMOSPHERIC TRANSMISSION)
5630 1) FORMAT(1H ,15X,11HWAVE NUMBER,5X,17HSPECTRAL RESPONSE)
5631 1) FORMAT(1H ,15X,E8.2,15X,E6.4)
5632 1) FORMAT(1H0,10X,4HTEMP,10X,4HNBAR)
5633 1) FORMAT(1H ,8X,F6.2,8X,F12.6)
5634 1) FORMAT(1H0,13HSURFACE LAYER,5X,4HNBAR,10X,3HTBB)
5635 1) FORMAT(1H1,10X,62HOUTGOING ATMOSPHERIC RADIATION)
1
5636 1) FORMAT(1H0,18A4)
5637 1) FORMAT(1H ,3I10,2F10.2)
5638 1) FORMAT(1H ,2E9.3,2(1X,E12.6),2F8.2,5(1X,F12.6))
5639 1) FORMAT(1H0,F10.2,F10.2,110)
5640 1) FORMAT(1H0,05X,13.2 MICRON H2O GEN ABSORP)
5641 1) FORMAT(1H0,05X,14.3 MICRON CO2 GEN ABSORP)
5642 1) FORMAT(1H0,05X,13.3 MICRON CH4 ABSORP)
5643 1) FORMAT(6F10.2)
5644 1) GRD PAD,03X,SURF HT,01X,SURF TEMP,02X,GRD TRAN,03X,
1,GRD RAD,06X,TOT RAD,06X,PER TOT,07X,TBB,
1,02X,WAVE,03X,LAMRDA,05X,PHI)
5645 1) TOTAL VERTICAL CO2 CONTENT BY PRESSURE INTEGRATION
1
5646 1) FORMAT(1H ,05X,2F10.3,05X,1PE14.6,05X,0PE10.4,F20.4,110)
5647 1) FORMAT(1H ,3(2X,F12.6,2X))
5648 1) FORMAT(1H1,11X,HU,10X,H1,06X,LAYER CONTRIB,05X,PER CENT OF
1ATM,05X,PER CENT OF TOT)
5649 1) FORMAT(1H0,10X,CM-ATM,NTP,10X,TOTAL CO2 PATH = ,F7.3,2X,PR-CM,15X,TOTAL O3 P
1ATH = ,F7.3,CM-ATM,NTP)
1P)
UNDER = 1.E-30
UNDER = UNDER*UNDER
WRITE(3,5601)
DATE--TABLE OF WAVE NUMBER VS LOG10(GEN ABS COEFF), IZE--TOTAL NO**
READ(2,3) IXE
WRITE(3,5610)
WRITE(3,5613)
DATE--TABLE OF LOG(L*U) VS TRANSMITTANCE; IZF--TOTAL NO OF POINTS

```



```

C      4.  WRITE(3,5612) (XLUU(I),DATUV(I),I=1,IXUU) *****
C      READ(2,5610) (WAVEV(I),DATV(I),I=1,IXV) *****
C      WRITE(3,5641) (WAVEV(I),DATV(I),I=1,IXV) *****
C      4.  READ(2,5612) LOG(L*U) VS TRANS*****
C      READ(2,5610) (XLUU(I),DATUV(I),I=1,IXVV) *****
C      WRITE(3,5612) (XLUU(I),DATUV(I),I=1,IXVV) *****
C      3.  READ(2,5612) WAVE NUMBER VS WEE*****
C      READ(2,5643) (WAVEW(I),WEE(I),I=1,IXW) *****
C      WRITE(3,5642) (WAVEW(I),WEE(I),I=1,IXW) *****
C      READ(2,8) (SPWGRD(I),I=1,18) *****
C      READ(2,3) (PHI *****
C      READ(2,5625) (WAVSP(I),PHI(I),I=1,IPHI) *****
C      READ(2,3) (IPAR *****
C      DO 9020 I=1,IPAR *****
C      READ(2,5626) XNBAR(I), TEMPBB(I) *****
C      WRITE(3,5626) XNBAR(I), TEMPBB(I) *****
9020 CONTINUE *****
C      READ(2,5611) WAVEI,DWAVE,INTER *****
C      WRITE(3,5639) WAVEI,DWAVE,INTER *****
C      XINTER=LOCAT(INTER) *****
C      WAVEF=WAVEI + XINTER*DWAVE - 5. *****
C      IATM=0 *****
C      NUM1=0.0 *****
C      HT2=0.0 *****
C      READ(2,3) NUM *****
C      NUU=NUM *****
C      READ(2,3) JTAN *****
C      READ(2,50) RAD,XMINH,DELR,HI,HT4,LAYER1,LAYER2,THLAY1,THLAY2,THLAY3 *****
C      READ(2,10) (ANGLE(I),I=1,JTAN) *****
C      READ(2,8) (WGRDS(I),I=1,18) *****
C      READ(2,13) GCDUM,P0,XMOL,PD,TO *****
C      READ(2,23) XMOL,C1H2,C2H2O,IGAS *****
C      CNH2C=XMOL/(12.4519*18.) *****
C      CNCO2=C1CO2/C2CO2,JGAS *****
C      CNCO2=CNCO2*(1.E+05) *****
C      READ(2,23) CNCO3,C1O3,C2O3 *****
C      CNCO3=CNCO3*(1.E+05) *****
C      CH4=2.4PPM(BCWMAN),1.1PPM(GOLDBERG), AVERAGE = 1.75PPM*****
C      CH4=(1.75E-6)*(1.E+05) *****
C      CN2C=(1.028E-06)*(1.E+05) *****
C      IDLEVEL = 50 *****

```



```

120 I=1,IXA
120 IXA=IXA+1-I
120 IXA1=2*I-1
120 IXA2=2*I
120 DATA(IXA1)=HH(IXAA)
120 DATA(IXA2)=TEMP(IXAA)
120 PRESS(I)=PRESS(IXAA)
120 PREHH(I)=1013.25*PRESH(I)
120 WRITE(3,35)I,IXAA,IXA1,IXA2,PRESH(I),DATA(IXA1),DATA(IXA2),PREH
120 I=1,IXA
120 CONTINUE
120 IXX=2*IXA
120 IH=HMIN(IXA)
120 HT4=HT4
120 HT=HT4
120 WRITE(3,36) IH,HT4,IH,HT
120 IXA=2*IXA
120 IATR=TABLE OF H VS H2O DIST, IXB-TOTAL NO OF POINTS*****
120 CONTINUE
120 WRITE(3,28) (HETH2O(I),QQH2O(I),I=1,IXB)
120 DATTC=TABLE OF H VS O2 DIST,IXC-TOTAL NO OF POINTS*****
120 WRITE(3,28) (HETCO2(I),QOCO2(I),I=1,IXC)
120 READ(2,3) IUP
120 READ(2,32) (HROT(I),I=1,IUP)
120 JTA=1
120 ANG=ANGLE(JTA)*0.017453294
120 IATA=0
120 NUM1=NUM1+1
120 IDELR1=(DELR*1000./2.)*.05
120 IHO=(RAD+XMINH)*SIN(ANG)
120 SUM=0.
120 SUMROT=0.
120 PRESSURE=0.
120 PREITER(3,5601)
120 IDELR=0
120 N=1
120 IHS=(HS+.0005)*1000.
120 IH=IH+IDELR
120 IH1=IH+IDELR+IDELR1
120 IDELP=DELR*1000+.5
120 X(N)=FLCAT(IH)/1000.
120 X1(N)=FLCAT(IH1)/1000.
120 DEL=DELL
120 HI=X1(N)

```



```

608 H=X(N)          TINAS(H1,HETTEM,TEMP,IXA,1)
      THBOT=TINAS(H,HETTEM,TEMP,IXA,1)
      XT1(N)=TH1
      XT2(N)=THBOT
      GR=GO*(RAD/(H1+RAD))**2
      GRBOT=GO*(RAD/(H+RAD))**2
      IF=(N.GT.1) GO TO 609
      PZRL = DELP/2
      SUM=SUM+PZRL*(GR*XVOL)*(1.E+05)/(RD*TH1)
      GO TO 607
609 CONTINUE
      SUM=SUM+DELL*(GP*XVOL)*(1.E+05)/(RD*TH1)
      SUMBOT=SUMBOT + DEL *(GRBOT*XVOL)*(1.E+05)/(RD*THBOT)
607 CONTINUE
      XP(N)=PI*(2.71828182**(-SUM))
      XPBOT(N)=PI*(2.71828182**(-SUMBOT))
      R=RAD+X(N)
      IE=(P-R)/610,610,612
610 R=RO
      RH=RO-ROO
      IH=H*1000.
      GO TO 605
612 XDEL(N)=(R/SORT(R**2-RO**2))*DELL
      IHT=(HT-DELE)*1000.
      N=N+1
      IF ( N - IVERIN ) 605,604,604
604 NGLAY=N-1
      HT4=X(NGLAY)
      HT = HT4
      HT3=HT4
      WRITE(3,5638) HT4
      IPR1=0
      IPR2=IPR1+55
      WRITE(3,29)
      WRITE(3,14) NUM1
      WRITE(3,18) (WORD(I),I=1,18)
      WRITE(3,9) (ANGLE(JTA),XMINH,HT2
      WRITE(3,6) (CONH20,C1H20,C2H20
      WRITE(3,25) (CONC02,C1C02,C2C02
      WRITE(3,5618) (CON03,C103,C203
      WRITE(3,40)
      WRITE(3,41) GO,PI,TO,RAD,RO,DELP,IGAS,JGAS,IATM,JTAN
      WRITE(3,24)
      DELE=0.
      TSUM1=0.
      TSUM1=0.
      SUM2=0.

```



```

C
UDELU = 0.0
UDELU2 = 0.0
UDELUU = 0.0
PDELUU = 0.0
TSUM2 = 0.0
PSUM2 = 0.0
SUM22 = 0.0
SUM4 = 0.0
SUM144 = 0.0
SUM222 = 0.0
SUM444 = 0.0
SUMCC2 = 0.0
DECC21 = 0.0
DECC2 = 0.0
SUMC = 0.0
SUMC4 = 0.0
SUMCH4 = 0.0
SUMN2C = 0.0
OPTICAL DEPTH COMPUTATION*****
DO 650 N=1,NCLAY
N=NCLAY-M+1
H=X(N)
H1=X1(N)
TH1=XT1(N)
PR=XP(N)
PRATIO=PR/PO
DELS=XDEL(N)
RHCI=XTINAS(H1,HETH2C,QQH2C,IXB,1)
RHJJ=XTINAS(H1,HETH2C,QQCQ2,IXC,1)
WATER=VAPOR OPTICAL PATH LENGTH*****
CALL PPELV(RHCI,PR,IGAS,CQNH2C,PEFF1)*****
SUM4=DELS*RHCI*((TO/TH1)**C1H2C)**C2H2C)*****
DELU1=SUM4*CQNH2C*****
DELU=DELU+DELU1*****
USUM4=DELS*RHCI*((PR/PO)*****
UDELU1=USUM4*CQNH2C*****
UDELU=UDELU+UDELU1*****
TSUM1=TH1*DELU1+TSUM1*****
PSUM1=PEFF1*DELU1+PSUM1*****
SUM2=SUM2+SUM4*****
DEPT1=CQNH2C*SUM2*****
AVEPI=TSUM1/DELU*****
AVERAGE=PSUM1/DELU*****
CZQNJ=OPTICAL PATH LENGTH**C1C3*****C2C3)*****
SUM44=DELS*RHJJ*****
DELU2=SUM44*CQNH2C*****
DELUU=DELU+DELU2*****
USUM44=DELS*RHJJ*****

```



```

1849 GO TO 1859
      IF(WAVEO.GE.2496.)GO TO 1851
      TRN20(N)=1.-((11.5*XTA(10,N,JTA))/70.)
      GO TO 1859
1851 IF(WAVEO.GE.2518.) GO TO 1853
      TRN20(N)=1.0
      GO TO 1859
1853 IF(WAVEO.GE.2608.) GO TO 1855
      TRN20(N)=1.0-((4.*XTA(10,N,JTA))/90.)
      GO TO 1859
1855 TRN20(N)=1.0
1859 CONTINUE
1861 REDH20=XTA(4,N,JTA)
      REDC02=XTA(8,N,JTA)
      XLUH63=ALOG10(REDH20)+GENH63
      XLUR02=ALOG10(REDH20)+GENR02
      XLUC02=ALOG10(REDC02)+GENC02
      XLUH32=ALOG10(REDH20)+GENH32
      XLUC43=ALOG10(REDC02)+GENC43
      RED03=XTA(7,N,JTA)
      IF(RED03-0.00) 808,808,809
      XLUC96=-15.
      GO TO 811
808 XLUC96=ALOG10(RED03)+GEN096
809 CONTINUE
811 XLUH63(N)=TINAS(XLUH63,XLUF,DATF,IXF,1)
      TRUR02(N)=TINAS(XLUR02,XLUH,DATH,IXH,1)
      ARGU=-EXP(ARGU)
      TRCON(N)=EXP(ARGU)
      TRC096(N)=1.
      CALL OZONE(WAVEO,REDH20,XTA(6,N,JTA),TRO96(N),2)
      TRC02(N)=TINAS(XLUC02,XLUN,DATN,IXN,1)
      TRH32(N)=TINAS(XLUH32,XLUU,DATUU,IXUU,1)
      TRC43(N)=TINAS(XLUC43,XLUV,DATUV,IXVV,1)
      WEC=33
      TRCH33(N)=EXP(-(XTA(9,N,JTA)/WEC)*0.56)
      TRAM(N)=TRC43(N)*TRH32(N)*TRCH33(N)*TRN20(N)
      TRAM(N)=TRC02(N)*TRO96(N)*TRR02(N)*TPH63(N)
      TRAM(N,J)=TRAM(N)
715 CONTINUE
      KIKI=KIKI+1
      WA(KIKI)=WAVEO
      GO TO (805,810,815,820,825,830,835,840,845,850,855,860,865,870,
1875),KIKI
805 DO 807 N=1,LA
807 TI(N)=TRAM(N)
      GO TO 716

```

C


```

810 DO T2(N)=TRAM(N)
812 DO T3(N)=TRAM(N)
815 DO T4(N)=TRAM(N)
817 DO T5(N)=TRAM(N)
820 DO T6(N)=TRAM(N)
822 DO T7(N)=TRAM(N)
825 DO T8(N)=TRAM(N)
827 DO T9(N)=TRAM(N)
830 DO T10(N)=TRAM(N)
832 DO T11(N)=TRAM(N)
835 DO T12(N)=TRAM(N)
837 DO T13(N)=TRAM(N)
840 DO T14(N)=TRAM(N)
842 DO T15(N)=TRAM(N)
845 DO T16(N)=TRAM(N)
847 DO T17(N)=TRAM(N)
850 DO T18(N)=TRAM(N)
852 DO T19(N)=TRAM(N)
855 DO T20(N)=TRAM(N)
857 DO T21(N)=TRAM(N)
860 DO T22(N)=TRAM(N)
862 DO T23(N)=TRAM(N)
865 DO T24(N)=TRAM(N)
867 DO T25(N)=TRAM(N)
870 DO T26(N)=TRAM(N)
872 DO T27(N)=TRAM(N)
875 DO T28(N)=TRAM(N)
877 DO T29(N)=TRAM(N)
      WRITE(3,5629) (WA(I),I=1,15)
      WRITE(3,905) XTA(1,N,JTA),T1(N),T2(N),T3(N),T4(N),T5(N),T6(N),T7(N),
      1,T8(N),T9(N),T10(N),T11(N),T12(N),T13(N),T14(N),T15(N),
      KIKI=0.0
716 CCNTINUE

```



```

1049 SUMLAY(I) = 0.0
      SUMR = 0.0
      SUMGRF = 0.0
      IF(IFRT1)1008,1008,1007
1007 WRITE(3,5644)
1008 CONTINUE
      DO 1050 K=1,INTER
      WAVEO = WAW(K)
      PHI = TINAS(WAVEO,WAVSP,PHI,IPHI,1)
      IF(PHI) 1050,1050,1009
1009 DO 1010 M=1,LA-M
      MZ = LA + 1 - M
      TRANV(M) = TRAMM(MZ,K)
      HET(M) = XTA(1,MZ,JTA)
      TOP LAYER*****
      PUP = 0.0
      TRANU = 1.0
      ITRANU = (TPANU + .000005)*100000.
      HU = HINTEG(1)
      HL = HINTEG(2)
      TPANL = TINAS(HL,HET,TRANV,LA,1)
      ITRANL = (ITRANL + .000005)*100000.
      TH = TMIDIN(1)
      CALL PLANK(WAVEO,DWAVE,TH,BBFW,BBFWQ)
      ITRAN = ITRAT(ITRANL)
      DTRAN = FLOAT(ITRAN)/100000
      TPANL = FLOAT(ITRANL)/100000.
      ITRANU = FLOAT(ITRANU)/100000.
      OLIVER = DIRAN*BBFW*PHI
      SUM = OLIVER + OLIVER
      SUMHTU(1) = HU
      SUMHTL(1) = HL
      SUMLAY(1) = SUMLAY(1) + OLIVER
      WAV = WAVEO
      IF(IFRT) 1870,1870,1865
1865 WRITE(3,5638)HU,HL,TRANU,TRANL,TH,WAV,BBFW,CLIVER,SUM,DTRAN,DTRA
      INI
      C ATMOSPHERIC LAYER S*****
1870 OLIVER = OLIVER - 2
      DO 900 M=1,OLIVER
      HU = HINTEG(M+1)
      HL = HINTEG(M+2)
      TH = TMIDIN(M+1)
      TRANU = TRANL
      ITRANU = ITRANL
      ITRANL = TINAS(HL,HET,TRANV,LA,1)
      ITRANL = (ITRANL + .000005)*100000.

```



```

CALL PLANK(WAVEO,DWAVE,TH,BBFW,BBFWO)
IDTRAN = ITRANU - ITRANL
DTRAN = FLOAT(IDTRAN)/100000
TRANL = FLOAT(ITRANL)/100000
TRANU = FLOAT(ITRANU)/100000
OLIVER = DTRAN*BBFW*PHI
SUM = SUM + OLIVER
SUMR = SUMR + OLIVER
SUMHTU(M+1) = HU
SUMHTL(M+1) = HL
SUMLAY(M+1) = SUMLAY(M+1) + OLIVER
WAV = WAVEO
IF(IPRT) 1880,1880,1875
IF(IWRITE(3,5638)HU,HL,TRANU,TRANL,TH,WAV,BBFW,OLIVER,SUM,DTRAN,DTRA
1875 INI
1880 IF(HL-HROT(J)) 901,901,900
900 CONTINUE
901 CONTINUE
RADATM = SUM
C SURF CONTRIBUTION*****
H = HL
TH = TINAS(H,HETTEM,TEMP,IXA,1)
TRAN = TINAS(H,HET,TRANV,LA,1)
CALL PLANK(WAVEO,DWAVE,TH,BBFW,BBFWO)
RADGRD = TRAN*BBFW*PHI
RADATM = RADATM + RADGRD
SUMGRD = SUMGRD + RADGRD
PER = RADATM/RA
CA = 1.1999-12
CB = 1.43879
TPR = (CB*WAV)/ALOG(DWAVE*CA*WAV**3/RA+1.0)
XXLAM = 1.f+04/WAV
IF(IPRT1) 1050,1050,1040
IF(IWRITE(3,5627)H,TH,TRAN,PAADGRD,PAADATM,RA,PER,TBB,WAV
1040 IWRITE(3,5627)H,TH,TRAN,PAADGRD,PAADATM,RA,PER,TBB,WAV
1050 1,XXLAM,PHI
CONTINUE
TOT = SUMR + SUMGRD
TBB = TOT*1.f+04
TBBR = TINAS(TOT,XNBAR,TEMPBB,IBAR,1)
WRITE(3,5634)
IWRITE(3,5627)H,1093,1093,TOT,TBBB
IF(IPRT2) 1100,1093,1093
IVV = IVER + 1
WRITE(3,5648)
IWRITE(3,11)IVV
DO 1097 JL=1,IVV
PERT = SUMLAY(JL)/(SUMR+SUMGRD)
PERT = SUMLAY(JL) / SUMR

```



```

1097 WRITE(3,5646) SUMHTU(JL),SUMHTL(JL),SUMLAY(JL),PERR,PERT,JL
1100 CONTINUE
1101 CONTINUE
      NUM=NUM-1
      IF(NUM) 710,710,20
1173 CONTINUE
710 STOP
      END

      SUBROUTINE CZONE(WAVEO,XMASS,PBAR,TAU,IFIRST)
      DIMENSION SDD(30),ADD(30),WAV(30),XKK(30)
      GO TO (50,90),IFIRST
50 CONTINUE
      READ(2,103) (ADD(I),I=1,27)
103 READ(2,103) (XKK(I),I=1,27)
      FORMAT(14F5.1)
      TAU=1.
      RETURN
90 CONTINUE
      PO=1013.25
      PI=22.77.
      IPT1=-1
      WAV(1)=940.
      WAV(27)=1100.
      DO 130 K=2,26
130 WAV(K)=955.
      + FLQAT(K-1)*5.
      SDD(1)=.004
      SDD(2)=.018
      SDD(3)=.036
      SDD(4)=.068
      SDD(5)=.120
      SDD(6)=.211
      SDD(7)=.376
      SDD(8)=.687
      SDD(9)=1.15
      SDD(10)=1.82
      SDD(11)=2.82
      SDD(12)=4.07
      SDD(13)=5.89
      SDD(14)=7.24
      SDD(15)=8.13
      SDD(16)=8.13
      SDD(17)=7.24
      SDD(18)=6.03
      SDD(19)=6.03
      SDD(20)=10.11
      SDD(21)=10.115

```



```

SDD(22)= 8.710
SDD(23)= 3.388
SDD(24)= 0.603
SDD(25)= 0.115
SDD(26)= .043
SDD(27)= .01
IF(IPRT1) 146,142,142
DO 145 J=1,27
WRITE(6,104)J,WAV(J),SDD(J),ADD(J),XKK(J)
104 FORMAT(1H,110,4F10.4)
WRITE(6,105)
105 FORMAT(1H,06X,4H WAVE,08X,1HK,07X,3HS/D,07X,3HA/D,07X,3HAZZ,08X,
12HAZ,08X,2HBZ,07X,3HAXX,08X,2HAX,07X,3HTAU)
146 CONTINUE
IF(WAVF0-940.) 150,155,155
150 TAU=1.0
GO TO 305
155 IF(WAVF0-1100.) 165,165,160
160 TAU=1.05
GO TO 305
165 XKK=TINAS(WAVE0,WAV,XKK,27,1)
SC=TINAS(WAVE0,WAV,SDD,27,1)
AD=TINAS(WAVE0,WAV,ADD,27,1)
AZZ=XMAS*SD/(PI*AD*(PBAR/PO))
AZ={XMASS*SD}/SQRT(1.+AZZ)
BZ=SQRT(ABS(XKK))
IF(XKK) 200,255,250
200 AXX=SIN(BZ*AZ)
GO TO 300
250 AXX= SINH(BZ*AZ)
AXX=AXX/(BZ*AZ)
GO TO 300
255 AXX=1.0
AXX=333.
300 CONTINUE
TAU=EXP(-AZ)*AX
305 CONTINUE
IF(IPRT1) 400,306,306
306 WRITE(6,100)WAVE0,XKK,SD,AD,AZZ,AZ,BZ,AXX,AX,TAU
100 FORMAT(1H,10F10.4)
400 CONTINUE
RETURN
END

```



```

SUBROUTINE PPEFV(RHO,PR,IGAS,CAPK,PEFF)
PR1=1.3
PR2=6.3
IF(IGAS-2) 10,20,30
PEFF=PR+(PR1-1.)*CAPK*10.**(-5)*PR
GO TO 40
PEFF=PR+(PR2-1.)*10.**(-3)*RHO*12.45*CAPK*PR
GO TO 40
PEFF=PR
RETURN
END
10
20
30
40

```

```

SUBROUTINE PLANK(WAVEO,DWAVE,TH1,PAOW,RADW)
DIMENSION PLK(5)
CA = 1.190SE-12
CB = 1.43879
PAOW=0.
RADW=0.
DW=NAVF0-2.0*DWAVE/5.0
DO 21 I=1,5
PLK(I) = CA*DW**3/(EXP(CB*DW/TH1)-1.0)
SE = 1.
RADW=RADW+PLK(I)*SE
PAOW=PAOW+PLK(I)
DW=DW+DWAVE/5.
CONTINUE
RETURN
END
18
21

```

```

FUNCTION TINAS ( A, X, Y, NX, KX )
L 0 0 2 3 0

```

```

AITKENS INTERPOLATION / EXTRAPOLATION
A = ARGUMENT
X = TABLE OF X'S
Y = TABLE OF Y'S
NX = NUMBER OF ENTRIES IN TABLE 'X'
KX = ORDER OF INTERPOLATION
NOTE: X(I) MUST BE LESS THAN X(I+1)
REAL *4 TINAS, A, X, Y, CX, CY
DIMENSION X(2), Y(2), CX(15), CY(15)

```

CCCCCCCCCCCCCCCC


```

C C      K = NO. POINTS TO USE
C C      KX = KX + 1
C C      IF( K .GT. 15) K = 15
C C      FIND NEAREST X(I)
C C      DO 10 I = 1, NX
C C      IF( A .LE. X(I) ) GO TO 20
C C      CONTINUE
C C      10 I = NX
C C      CHECK FOR EVEN/ODD NO. POINTS
C C      20 IF( MOD(K,2) .EQ. 1 ) GO TO 40
C C      SET I SO PTS X (I) TO X(I+KX) = NEAREST POINTS TO 'A'
C C      30 I = I - K/2
C C      IF( I .LT. 1 ) I = 1
C C      IF( I .GT. NX ) I = NX - K + 1
C C      GO TO 50
C C      K IS ODD. SET I SO MIDDLE POINT IS NEAREST TO 'A'
C C      40 IF( I .EQ. 1 ) GO TO 50
C C      J = I - 1
C C      IF( A .LE. ( X(I) + X(J) ) * 0.5 ) I = J
C C      GO TO 30
C C      SET INITIAL CY, CX
C C      50 DO 60 J = 1, K
C C      CX(J) = X(I) - A
C C      CY(J) = Y(I)
C C      I = I + 1
C C      PERFORM INTERPOLATION
C C      M = K - 1
C C      DO 80 J = 1, M
C C      DO 70 I = J, M
C C      70 CY(I+1) = ( CX(I+1)*CY(J) - CX(J)*CY(I+1) ) / (CX(I+1) - CX(J))
C C      80 CONTINUE
C C      TINAS = CY(K)
C C      RETURN

```


LIST OF REFERENCES

- Belmont, A. D., G. W. Nicholas and W. C. Shen, 1968: Comparison of 15- μ TIROS VII Data with Radiosonde Temperatures. Journal of Applied Meteorology, 7, 284-289.
- Dixon, W. J., (Ed.), 1966: Biomedical Computer Programs, Health Sciences Computing Facility, University of California at Los Angeles, 585 pp.
- Dubin, M., Sissenwine, N. and Teweles, S., 1966: U. S. Standard Atmosphere Supplements, 1966, National Science Services Administration, National Aeronautics and Space Administration and United States Air Force, 289 pp.
- Kennedy, J. S., 1966: An Atlas of Stratospheric Mean Isotherms Derived From TIROS VII Observations, 85 pp.
- Kunde, V. G., 1967: Theoretical Computations of the Outgoing Infrared Radiance from a Planetary Atmosphere, 117 pp.
- Meteorological Analyses, Institute for Meteorology and Geophysics of the Free University of Berlin, January-March 1964.
- Miller, R. G., 1962: Statistical Prediction by Discriminant Analysis, Meteor. Monogr., 4, No. 25, Boston, Mass., Amer. Meteor. Soc., 53 pp.
- Nordberg, W., 1966: Satellite Radiation Measurements in Spectral Regions. Satellite Data in Meteorological Research, National Center for Atmospheric Research, NCAR-TN-11, Boulder, Colo., 199-213.
- Shen, W. C., G. W. Nichols and A. D. Belmont, 1968: Antarctic Stratospheric Warming During 1963 Revealed by 15- μ TIROS VII Data. Journal of Applied Meteorology, 7, 268-283.
- Teweles, S., 1966: Radiometer data in the 15- μ band. Satellite Data in Meteorological Research, National Center for Atmospheric Research, NCAR-TN-11, Boulder, Colo., 251-257.
- Staff Members. 1965: TIROS VII Radiation Data Catalog and Users' Manual. National Space Science Data Center, Greenbelt, Md., 269 pp.
- Warnecke, G., 1967: The Remote Sensing of Stratospheric Temperatures and Some Results From the Nimbus II Satellite Experiment, Goddard Space Flight Center, Greenbelt, Md., 24 pp.

INITIAL DISTRIBUTION LIST

	No. Copies
1. Lieutenant Commander Larry L. Giauque Fleet Weather Central Box 2 COMNAVMARIANAS FPO San Francisco, 96630	2
2. Professor Frank L. Martin Department of Meteorology Naval Postgraduate School Monterey, California 93940	6
3. Department of Meteorology Naval Postgraduate School Monterey, California 93940	3
4. Library, Code 0212 Naval Postgraduate School Monterey, California 93940	2
5. Defense Documentation Center Cameron Station Alexandria, Virginia 22314	2

DOCUMENT CONTROL DATA - R & D

(Security classification of title, body of abstract and indexing annotation must be entered when the overall report is classified)

1. ORIGINATING ACTIVITY (Corporate author)

Naval Postgraduate School
Monterey, California 93940

2a. REPORT SECURITY CLASSIFICATION

Unclassified

2b. GROUP

3. REPORT TITLE

Calculation of Levels of Relative Contribution of the Carbon-dioxide
Channel Radiance from TIROS VII in the Case of a Large-scale
Stratospheric Warming in January 1964

4. DESCRIPTIVE NOTES (Type of report and inclusive dates)

Master's Thesis; September 1971

5. AUTHOR(S) (First name, middle initial, last name)

Larry Lee Giauque

6. REPORT DATE

September 1971

7a. TOTAL NO. OF PAGES

62

7b. NO. OF REFS

12

8a. CONTRACT OR GRANT NO.

b. PROJECT NO.

c.

d.

9a. ORIGINATOR'S REPORT NUMBER(S)

9b. OTHER REPORT NO(S) (Any other numbers that may be assigned
this report)

10. DISTRIBUTION STATEMENT

Approved for public release; distribution unlimited.

11. SUPPLEMENTARY NOTES

12. SPONSORING MILITARY ACTIVITY

Naval Postgraduate School
Monterey, California 93940

13. ABSTRACT

A case study of a winter stratospheric warming in the western hemisphere in January 1964 between 60° and 40° north latitudes was conducted. Utilizing TIROS VII radiance data and analyzed height fields, a stepwise regression equation was determined to specify lower stratospheric layer temperatures. These temperatures were used with standard atmospheric temperatures to construct a sounding for use in a radiance computer program. Finally, this computed radiance was compared to regression values to determine if prediction and study of stratospheric warmings are valid and useful.

KEY WORDS

LINK A

LINK B

LINK C

ROLE

WT

ROLE

WT

ROLE

WT

Stratospheric Warming

Channel Radiance

Stratospheric layer temperatures

TIROS VII radiance data

BINDERY

Thesis

G35

c.1

Giauque

131315

Calculation of levels of relative contribution of the carbon-dioxide channel radiance from TIROS VII in the case of a large-scale stratospheric warming in January 1964.

Thesis

G35

c.1

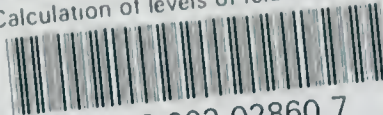
Giauque

131315

Calculation fo levels of relative contribution of the carbon-dioxide channel radiance from TIROS VII in the case of a large-scale stratospheric warming in January 1964.

thesG35

Calculation of levels of relative contri



3 2768 002 02860 7

DUDLEY KNOX LIBRARY